Synthesis of Ternary Nanocomposites of MnO_2/PANI/Maxsorb and their Performance as an Electrode Material for Supercapacitors

Aprilianti Nur'aini[1,2], Imam Prasetyo[1,2] & Teguh Ariyanto[1,2,*]

[1]Department of Chemical Engineering, Faculty of Engineering, Universitas Gadjah Mada, Jalan Grafika No. 2 UGM, 55281, Yogyakarta, Indonesia
[2]Carbon Materials Group Research, Chemical Engineering Department, Faculty of Engineering, Universitas Gadjah Mada, Jalan Grafika No. 2 UGM, 55281, Yogyakarta, Indonesia
*E-mail: teguh.ariyanto@ugm.ac.id

Abstract. Increasing performance of supercapacitors can be achieved by using a composite of electrode materials. Nevertheless, selecting appropriate materials and determining the optimal combination composition remain significant challenges. In this research, a ternary composite of MnO_2/polyaniline (PANI)/Maxsorb was studied. The combination of Maxsorb, PANI, and MnO_2 is a unique feature of this research, with Maxsorb acting as a porous structural framework; PANI enhancing electrical conductivity; and MnO_2 providing high pseudocapacitance. The ternary material was prepared by impregnation of MnO_2 and PANI into the pores of Maxsorb carbon in a two-sequence procedure, i.e., (i) incipient wetness impregnation of $Mn(NO_3)_2$ into porous carbon followed by calcination to obtain MnO_2/Maxsorb, and (ii) *in situ* polymerization of aniline monomer in the MnO_2/Maxsorb, hence obtaining the final ternary nanocomposite of MnO_2/PANI/Maxsorb. The electrochemical test using H_2SO_4 electrolyte (1 M) revealed that the ternary material outperformed single porous carbon or PANI as well as their binary nanocomposite in terms of properties such as energy density, power density, and capacitance. The ternary material had a specific surface area of around 2,078 $m^2\ g^{-1}$, containing microporous and mesoporous structures. The material featured a specific capacitance up to 500 F g^{-1} and a power density of 37.6 kW kg^{-1} as well as an energy density of 62.69 Wh kg^{-1}.

Keywords: *manganese dioxide; Maxsorb; polyaniline; supercapacitor; ternary nanocomposite.*

1 Introduction

Supercapacitors are one of a kind in energy storage systems, featuring great density of power, rapid charge/discharge, and a high number of cycles, giving supercapacitors relatively longer service lives than batteries. Supercapacitors are

Received January 13th, 2025, Revised October 20th, 2025, Accepted for publication December 20th, 2025
 ISSN: 2337-5760, DOI: 10.5614/j.math.fund.sci.2025.57.2.2

known for their high power density, which gives them a significant performance advantage in a range of applications, including hybrid electric vehicles, pulsed laser systems, solar-powered street lighting, and power tools. This benefit arises from their capability to charge and discharge rapidly, a process governed by the speed of ion adsorption and movement within the porous structure as well as the electrical conductivity of the electrode materials. Supercapacitors are typically divided into two main categories: electric double-layer capacitors (EDLCs) and pseudocapacitors. EDLCs store charge via electrostatic interactions at the interface of porous materials, making their performance highly dependent on the electrode's surface area and pore size distribution. Porous carbon is a widely used material for EDLC electrodes. In contrast, pseudocapacitors store energy through reversible Faradaic redox reactions occurring at the surface, often employing transition metal oxides or conductive polymers. While EDLCs offer excellent power density and a long cycle life, they are limited by relatively low energy density and capacitance. Meanwhile, pseudocapacitors offer higher energy density but have lower electrical conductivity and poor cycling stability [1-4].

The rapid charge–discharge ability of supercapacitors strongly depends on the ion mobility within their porous structure and the electrical conductivity of the electrode materials. To achieve high performance, combining materials exhibiting both electric double-layer capacitance (EDLC) and pseudocapacitance has been widely explored [5]. Pure materials rarely possess both characteristics; thus, nanocomposites have been developed to integrate the advantages of different components. For instance, ternary composites such as AC/MnO_2/PANI have shown a specific capacitance of 245 F/g, outperforming AC/PANI (161.7 F/g) [6]. However, activated carbon (AC) often suffers from pore blockage when additional materials are incorporated, which can hinder ion transport and reduce capacitance.

To overcome this limitation, mesoporous carbon materials with larger pore diameters are preferred, as they facilitate faster ion diffusion and better capacitance retention compared to microporous carbons [7]. Among various candidates, Maxsorb carbon offers an exceptionally high surface area and a well-developed pore network, enabling efficient ion transport and high charge storage capacity [8]. While typical steam-activated carbon products exhibit surface areas of around 1,000 m^2/g, Maxsorb can achieve surface areas exceeding 2,000 m^2/g, indicating superior adsorption capability. These features make Maxsorb an ideal conductive framework for supporting pseudocapacitive materials such as polyaniline (PANI) and manganese dioxide (MnO_2). PANI provides high intrinsic electrical conductivity, fast and reversible redox reactions, and excellent charge–discharge rates, enhancing the overall conductivity and power performance of the electrode [9]. Meanwhile, MnO_2 contributes a high theoretical capacitance, large energy density, and environmental stability, allowing the

composite to store more charge through Faradaic redox processes [10]. The combination of Maxsorb, PANI, and MnO_2 is expected to produce a synergistic effect, with Maxsorb serving as a porous structural host, PANI enhancing electrical conductivity, and MnO_2 contributing high pseudocapacitance. This ternary nanocomposite is hypothesized to deliver superior energy and power densities as well as enhanced overall electrochemical performance compared to electrodes composed of single or binary materials.

In this study, a MnO_2/PANI/Maxsorb ternary nanocomposite was synthesized using *in situ* polymerization and wet impregnation to combine the conductivity of PANI, the Faradaic pseudocapacitance of MnO_2, and the high surface area of Maxsorb. The electrochemical performance of the ternary composite was evaluated in comparison with its binary and single-component counterparts to demonstrate the synergistic enhancement arising from this combination of materials.

2 Materials and Methods

2.1 Materials

The materials for the ternary nanocomposites were Maxsorb MSC30 purchased from Kansai Coke and Chemical Co., Ltd. (with ca. 3,000 m^2/g specific surface area, ca. 1.5 cm^3/g pore volume, ca. 2 nm mean pore size, >95% carbon content, and 100-200 μm particle size), H_2O_2 (30%, Merck) as oxidator, aniline (99.5%, Merck), ammonium persulfate or APS (technical grade, Merck), hydrobromic acid (48%, Loba Chemie), and $Mn(NO_3)_2.4H_2O$ (technical grade, Merck). The resulting nanocomposite was employed as the working electrode material, with platinum (Pt) serving as the counter electrode and Ag/AgCl (in a 3 M KCl solution) used as the reference electrode. The electrolyte used during the electrochemical measurement process was a 1 M H_2SO_4 solution. Other materials needed during the electrochemical measurement process were Nafion 117 as the binder and isopropanol as dispersant of the carbon ink.

2.2 Methods

2.2.1 Preparation of Ternary Materials

Maxsorb carbon was grinded to a size of under 400 mesh and chemically surface-oxidized using H_2O_2 15%. The activated carbon was then filtered and dried before being impregnated with $Mn(NO_3)_2.4H_2O$ that had been dissolved with 70% ethanol. The incipient wetness impregnation process for impregnating $Mn(NO_3)_2.4H_2O$ in Maxsorb carbon took place by dripping $Mn(NO_3)_2.4H_2O$ solutions over Maxsorb at room temperature and vacuum pressure. The amount

of $Mn(NO_3)_2.4H_2O$ solution used was adjusted to 5 or 10% of the weight of the Maxsorb carbon component. The resulting slurry was dried and then heated in a furnace at a temperature of 300 ℃ for 6 hours and a heating rate of 2 ℃/minute. The detailed procedure can be found in the literature [7]. This produced the binary nanocomposite MnO_2/Maxsorb.

The prepared MnO_2/Maxsorb nanocomposite was placed in a polymerization reactor with a solution of 5 or 10% weight aniline in 1 M HBr. The solution was then chilled to a temperature of 0 to 5 ℃ while being stirred continuously with a magnetic stirrer. Meanwhile, in a temperature range of 0 to 5 ℃, the carbon and aniline mixture was dripped with a 1 M HBr and APS solution to initiate the reaction. The polymerization reaction was carried out for 4 hours. The resulting MnO_2/PANI/Maxsorb ternary nanocomposite was filtered and washed using 1 M HBr and acetone. The binary composite of PANI/Maxsorb was prepared with a typical procedure.

2.2.2 Characterization of Materials

The main material characterizations included pore structure, microstructure, and functional group characterizations. The characterization of the material pore structure was performed through nitrogen sorption using a Quantachrome NOVA 2000 device. The specific surface area was measured using the Brunauer-Emmett-Teller (BET) technique. Meanwhile, the microstructural features and functional groups were analyzed using X-ray diffraction (XRD) with a Bruker D2 Phaser and Fourier-transform infrared spectroscopy (FTIR) with a Nicolet Avatar 360, respectively. Analysis using these methods resulted in diffraction (XRD) or transmittance (FTIR) patterns, respectively, with peaks that corresponded with certain crystalline microstructures and functional groups.

2.2.3 Electrochemical Measurements

The electrochemical measurement of the material-specific capacitance was determined using a three-electrode system. The working electrode was prepared by weighing 10 mg of the material to be tested. The sample was then mixed with 1 mL of isopropanol and 20 μL of Nafion 117. The resulting mixture was sonicated before being applied to the working electrode. The sonification process aims to homogenize the carbon ink before extraction using a micropipette. Homogenization is essential to ensure uniform dispersion of materials within the liquid, facilitating optimal conditions for subsequent testing. To complete the three-electrode setup, a platinum (Pt) counter electrode, an Ag/AgCl reference electrode, and a 1 M H_2SO_4 electrolyte solution were assembled. The capacitance of the material was measured using cyclic voltammetry methods with 5 to 100 mV s^{-1} as the scan rate and a potential window range from -0.40 V to 0.80 V.

3 Results and Discussion

3.1 Material Characteristics

3.1.1 Pore Structures

To evaluate the pore structure characteristics, a N_2-sorption analysis was performed. The methodology involved the examination of nitrogen adsorption and desorption isotherms; the resulting data is visually presented in Fig. 1A. This analytical approach shows the details of the material's porosity, providing valuable insights into its pore size distribution, surface area, and overall structural features.

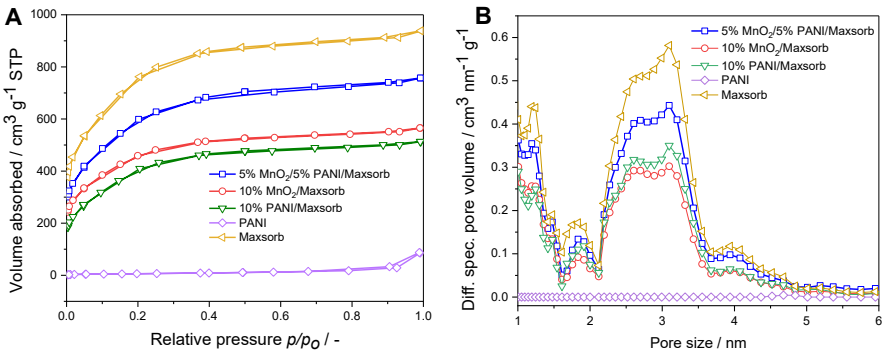

Figure 1 Nitrogen adsorption-desorption isotherms (A) and pore size distributions of the ternary composite of MnO_2/PANI/Maxsorb, the binary composites, and their references (B).

The nitrogen adsorption isotherms, as depicted in Fig. 1(A), outline the amount of nitrogen adsorbed by the material across a range of relative pressures. Based on the isotherm analysis, both the Maxsorb and the nanocomposite materials displayed type IB characteristics as classified by IUPAC, suggesting that the materials contained a significant amount of micropores with a broad distribution, along with the presence of mesopores [8]. The presence of mesopores is indicated by an increase in nitrogen volume absorbed at higher relative pressures (>0.2 P/P_o). Aside from the types of material pores, the surface area and volume of the pores can be estimated from the total volume of nitrogen being absorbed. Fig. 1(A) demonstrates that the material with the highest nitrogen adsorption capacity was the Maxsorb. With the impregnation of MnO_2 and PANI particles, the amount of absorbed nitrogen decreased. PANI impregnation resulted in a greater reduction in nitrogen adsorption compared to MnO_2.

The pore size distribution graph is shown in Fig. 1(B). From this graph, the percentage of pores for a given diameter for each material can be seen. Pure Maxsorb carbon could absorb the largest amount of nitrogen among all the materials that were tested in this study. This result indicates that both the number of micropores and mesopores decreased with the impregnation of PANI and MnO_2 into Maxsorb. This decrease is attributed to PANI and MnO_2 filling or even covering the pores of the Maxsorb. The reduction in micropores and mesopores due to the addition of PANI was much more significant than that caused by MnO_2. This is because PANI, being a conducting polymer, has a much larger size compared to MnO_2 [9]. Polyaniline typically forms nanorods or nanofibers with diameters of around 80 nm [23], whereas MnO_2 nanoparticles or nanorods generally exhibit much smaller sizes, typically in the range of 10 to 40 nm [24,25].

Table 1 Summarized pore characteristics of ternary composite of MnO_2/PANI/Maxsorb, binary composites, and their references.

Sample	Specific Surface Area [m^2g^{-1}]	Mean Pore Diameter [nm]	Micropore Volume [%]	Pore Volume Total [cm^3g^{-1}]
5% MnO_2/5% PANI/Maxsorb	2078.74	2.25	55.42	1.17
10% PANI/Maxsorb	1422.38	2.23	53.40	1.45
10% MnO_2/Maxsorb	1597.49	2.19	58.90	0.87
PANI 100%	22.17	23.80	0.00	0.13
Maxsorb	2643.67	2.19	57.50	1.45

The decrease in pore size due to the impregnation of MnO_2 and PANI is also confirmed by the specific surface area (SSA) data in Table 1, where Maxsorb had the largest SSA value, at 2643.67 m^2/g, which is consistent with the literature [10]. The order of surface area values, from largest to smallest, starts with Maxsorb > 5% MnO_2/5% PANI/Maxsorb > 10% MnO_2/Maxsorb > 10% PANI/Maxsorb, and ends with PANI 100%.

3.1.2 Microstructures

The microstructure was analyzed using X-ray diffraction (XRD); the results are shown in Fig. 2(A). The XRD pattern of 10% PANI/Maxsorb shows a major peak at an angle of $2\theta = 22.96°$ and the peaks are also visible in the ternary material. The broad diffraction peak corresponding to the C (002) plane within the 2θ range of 15 to 30º is indicative of the presence of amorphous carbon. Additionally, the weak and wide peak observed around $2\theta = 40$ to 50º, associated with the C (101) plane, reflects the a-axis orientation of the graphite structure [11]. The PANI peak should appear at $2\theta = 19.31°$ and 25.72°, indicating low crystallinity as a

characteristic of conductive polymers due to the repetition of benzenoid and quinoid rings [12].

However, in the nanocomposites 10% PANI/Maxsorb and 5% MnO_2/5% PANI/Maxsorb, PANI did not have a significant effect on the diffraction pattern of Maxsorb because the PANI content is relatively low. On the other hand, both PANI peaks disappeared in the XRD pattern of the binary composite 10% MnO_2/Maxsorb and were replaced by smaller peaks at $2\theta = 35.85°$ and 59.6°, which correspond to the (100) and (110) planes of the MnO_2 particles [13]. This is likely due to the higher weight percentage of MnO_2 impregnated in the binary composite compared to the ternary composite. These MnO_2 peaks will disappear in the XRD pattern of ternary composites with lower weight percentages of MnO_2.

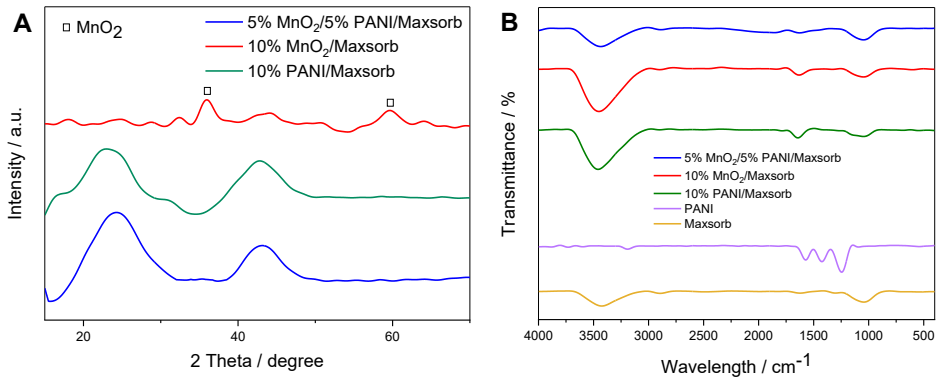

Figure 2 X-ray diffraction result (A) and FTIR spectrum result of the ternary composite of MnO_2/PANI/Maxsorb, the binary composites, and their references (B).

3.1.3 Functional Groups

The FTIR spectra of the materials are shown in Fig. 2(B). All materials, except for PANI, exhibited a peak at around 3,400 cm^{-1}, indicating the influence of activation using H_2O_2 on the FTIR spectra. From the formed peaks, the peak at a wavenumber of approximately 3,400 cm^{-1} indicates the presence of -OH stretching for alcohols and phenols in the solid phase [14]. The additional -OH groups on the material's surface after activation lead to increased hydrophilicity of the carbon material, making it easier to disperse in liquids. In 10% MnO_2/Maxsorb, the absorption bands at 1617 and 1047 cm^{-1} are associated with O-H bending vibrations coupled with Mn atoms. The presence of O–H vibrational bands in the FTIR spectrum indicates that water molecules are adsorbed within the MnO_2 structure. This hydration can facilitate cation mobility, which in turn may enhance the capacitance performance of MnO_2 [14,15]. The peak showing

MnO_2 is also visible at 1045 cm^{-1} in the 5% MnO_2/5% PANI/Maxsorb. In this study, there was no peak indicating Mn-O functional groups that should be present at 538 cm^{-1} [13]. On the other hand, the PANI exhibited several peaks distinct from MnO_2. The bands at 1,575 and 1,432 cm^{-1} are quinonoid (Q) and benzenoid (B) ring vibrations [17]. The characteristic of the conducting protonated is visible at 1,248 cm^{-1}, counted as corresponding to C–N stretching vibration [18]. The functional groups characterizing PANI are not visible in the 10% PANI/Maxsorb and 5% MnO_2/5% PANI/Maxsorb nanocomposites, because of the low PANI content in these nanocomposites.

3.2 Electrochemical Performances

The electrochemical properties of each constituent material, the binary nanocomposites, and the ternary nanocomposite were assessed using the three-electrode system method to obtain cyclic voltammetry graphs. These graphs depict the capacitance values of each material. Testing was conducted at various scan rates to understand the relationship between capacitance and applied scan rate. The capacitance values were also utilized to calculate the energy density and power density of each material. The obtained energy density and power density values were then plotted in a graph known as a Ragone plot, illustrating the relationship between energy density and power density. The electrochemical property values obtained from the testing served as evaluative data for the performance of each material as a supercapacitor electrode.

3.2.1 Cyclic Voltammetry (CV) Graphs

CV graphs can determine the type of supercapacitor by its size and shape. From the area generated in a CV graph, the capacitance value can be calculated. In Fig. 3(A), it can be observed that each material produced different CV shapes at a scan rate of 25 mV s^{-1}. Maxsorb exhibited a nearly rectangular charge/discharge shape, which characterizes the behavior of an electric double-layer capacitor (EDLC) with a capacitance value of around 194 F g^{-1}. The rectangular shape indicates efficient and unrestricted electrolyte ion transport within the pores of the Maxsorb, resulting in the formation of a stable and well-developed electric double layer [19]. On the other hand, the PANI generated a shape with peaks at the top and bottom. These peaks show the occurrence of Faradaic redox reactions, indicating the characteristics of pseudocapacitors. The top peak shows an oxidation reaction, while the bottom peak shows the reduction reaction. This redox peaks of the PANI increase the area, resulting in a capacitance value that is not significantly different from that of Maxsorb (ca. 113 F g^{-1}) [20].

The nanocomposite of 10% MnO_2/Maxsorb showed 238 F g^{-1} as the capacitance number and a shape close to rectangular with slight waves at the top and bottom, indicating peaks that signify Faradaic redox reactions generated by MnO_2. This

phenomenon is in agreement with observation in references when only using MnO_2 [26]. Materials of 10% PANI/Maxsorb and 5% MnO_2/5% PANI/Maxsorb exhibited higher peaks compared to 10% MnO_2/Maxsorb. This is because the larger size of PANI compared to MnO_2 means it can partially cover some of the Maxsorb pores. The widest charge/discharge cycle was possessed by 5% MnO_2/5% PANI/Maxsorb, indicating that the ternary nanocomposite had the highest capacitance among all materials, i.e., 500 F g^{-1} at a scan rate of 25 mV s^{-1}. The results of specific capacitance in this research were relatively superior compared to previous research of another ternary composite [5]. The electrochemical performance observed from the CV curves can be directly related to the microstructural characteristics revealed by the BET and XRD analyses. The higher surface area and suitable pore distribution (BET) provide more active sites for ion adsorption, while the crystalline structure and phase composition (XRD) influence the charge transfer behavior and overall capacitance performance.

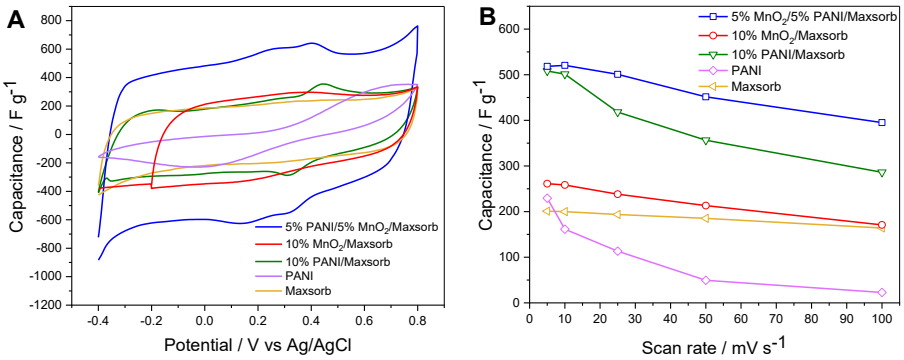

Figure 3 CV measurement at 25 mV s^{-1} (A) and capacitance vs scan rate of the ternary composite of MnO_2/PANI/Maxsorb, the binary composites, and their references (B).

The 5% MnO_2/5% PANI/Maxsorb electrode exhibited the widest CV curve and the highest capacitance of 500 F g^{-1} at a scan rate of 25 mV s^{-1} in 1 M H_2SO_4, indicating strong synergistic interactions among the MnO_2, PANI, and activated carbon. Compared with previous reports, its capacitance was lower than that of MnO_2-doped PANI/CNT, which achieved 1360 F g^{-1} at 5 mV s^{-1} [27], but higher than PANI/CNT, which showed 385 F g^{-1} at 0.5 A g^{-1} [28]. The differences are partly due to the variation in scan rate: lower scan rates allow sufficient ion diffusion into the electrode's porous structure, resulting in higher capacitance values, while higher scan rates limit ion accessibility, reducing charge storage efficiency. Despite being tested at a higher scan rate, the 5% MnO_2/5% PANI/Maxsorb composite still exhibited considerable capacitance, suggesting that its microstructure effectively facilitates ion transport. This is consistent with

the BET and XRD results, which indicate increased surface area and semi-crystalline phases that enhance ion diffusion and charge transfer during redox processes.

3.2.2 Capacitance vs Scan Rate

As the scanning rate increased, the ohmic resistance of electrolyte migration within the material pores also increased, resulting in smaller capacitance measurements. Fig. 3(B) demonstrates an inverse relationship between scanning rate and specific capacitance, where at low scanning rates, CV tended to yield higher capacitance, while at high scanning rates, CV yielded lower capacitance. It is believed that reducing the scanning rate allows the electrolyte to penetrate more evenly into the pores and make better contact with the internal surface of the electrode material, thereby resulting in higher capacitance. The linear dependence of capacitance on scanning rate indicates that ion transport is controlled by diffusion, which is also found in the literature [21].

3.2.3 Ragone Plot

The performance of supercapacitors can also be assessed through a Ragone plot, as shown in Fig. 4, which provides an overview of the relationship between energy density and power density. Among these materials, 5% MnO_2/5% PANI/Maxsorb exhibited an energy density peak at 103.7 Wh kg^{-1} and a power density of 1.6 kW kg^{-1}. However, at higher power levels, the energy density dropped rapidly, while the power density increased. When the power density of 5% MnO_2/5% PANI/Maxsorb reached 37.6 kW kg^{-1}, its energy density decreased by 40%.

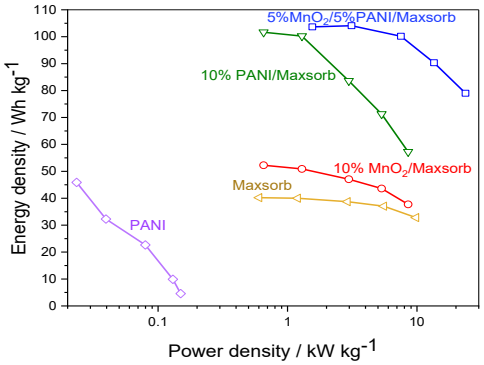

Figure 4 Ragone plot of the Maxsorb, PANI, and nanocomposites.

The 10% PANI/Maxsorb and 10% MnO_2/Maxsorb nanocomposite showed a lower number energy density of 101.7 Wh kg^{-1} and 36.3 Wh kg^{-1} as an impact of

their low specific surface areas. The decrease in energy density for 10% PANI/Maxsorb and 10% MnO_2/Maxsorb was much higher than the power density increase, respectively 60.28% and 53.99%, with a maximum power density of 24.2 kW kg^{-1} and 12 kW kg^{-1}. Based on capacitance, energy density, and power density, the 5% MnO_2/5% PANI/Maxsorb material demonstrated the best performance as a supercapacitor electrode. The results of energy and power density in this research surpass previous research of another nanocomposite of activated carbon [22].

4 Conclusions

A ternary nanocomposite of MnO_2/PANI/Maxsorb was successfully synthesized by impregnation of MnO_2 and *in situ* polymerization of polyaniline and the material was tested as an electrode material for supercapacitors. The characterization data (N_2 sorption, XRD, and FTIR) indicate that the ternary nanocomposite had a high surface area but lower than that of Maxsorb only. Furthermore, XRD and FTIR also showed the successful formation of MnO_2 and impregnation of PANI. As a supercapacitor electrode, MnO_2/PANI/Maxsorb nanocomposites showcase a beneficial combination of a high specific surface area of pores and great pseudocapacitive properties, which result in an excellent capacitance of 500 F g^{-1}. This ternary nanocomposite electrode showcased 62.69 Wh kg^{-1} energy density at 37.6 kW kg^{-1} power density. Hence, the ternary nanocomposite demonstrated potential in terms of extraordinary electrochemical properties and performance compared to each individual pure component.

5 Acknowledgements

The authors acknowledge funding through Department of Chemical Engineering Research Grant 2023 under no. 2790102/UN1.FTK/SK/HK/2023.

6 References

[1] Simon, P. & Gogotsi, Y., *Materials for Electrochemical Capacitors*, Nat. Mater., **7**(11), pp. 845-854, 2008.

[2] Su, F., Poh, C.K., Chen, J.S., Xu, G., Wang, D., Li, Q., Lin, J. & Lou, X.W., *Nitrogen-containing Microporous Carbon Nanospheres with Improved Capacitive Properties*, Energy Environ. Sci., **4**(3), pp. 717-724, 2011. doi: 10.1039/c0ee00277a.

[3] Jiang, J., Li, Y., Liu, J., Huang, X., Yuan, C. & Lou, X.W., *Recent Advances in Metal Oxide-based Electrode Architecture Design for Electrochemical Energy Storage*, Adv. Mater., **24**(38), pp. 5166-5180, 2012. doi: 10.1002/adma.201202146.

[4] Zhai, Y., Dou, Y., Zhao, D., Fulvio, P.F., Mayes, R.T. & Dai, S., *Carbon Materials for Chemical Capacitive Energy Storage*, Adv. Mater., **23**(42), pp. 4828-4850, 2011. doi: 10.1002/adma.201100984.

[5] Wibowo, J. F., Prasetyo, I. & Ariyanto, T., *PANI/Porous Carbon Palm Kernel Shell via In Situ Polymerization Method for Supercapacitor Electrode*, Solid State Phenom., **345**, pp. 123-130, 2023. doi: 10.4028/p-3A39kD.

[6] Chen, W., Tao, X., Wei, D., Wang, H., Yu, Q. & Li, Y., *High-Performance Supercapacitor based on Activated Carbon–MnO_2–Polyaniline Composite*, J. Mater. Sci. Mater. Electron., **27**(2), pp. 1357-1362, 2016. doi: 10.1007/s10854-015-3897-z.

[7] Nur'aini, A., Formulasi dan Karakterisasi Nanokomposit MnO_2/Polianiline/Maxsorb untuk Material Elektroda Superkapasitor, Bachelor Thesis, Department of Chemical Engineering, Universitas Gadjah Mada, Yogyakarta, 2023.

[8] Thommes, M., Kaneko, K., Neimark, A. V., Olivier, J.P., Rodriguez-Reinoso, F., Rouquerol, J., & Sing, K.S.W., *Physisorption of Gases, with Special Reference to the Evaluation of Surface Area and Pore Size Distribution (IUPAC Technical Report),* Pure and Applied Chemistry, **87**(9-10), pp. 1051-1069, 2015. doi: 10.1515/pac-2014-1117.

[9] Bednarczyk, K., Matysiak, W., Tański, T., Janeczek, H., Schab-Balcerzak, E. & Libera, M., *Effect of Polyaniline Content and Protonating Dopants on Electroconductive Composites*, Sci. Rep., **11**(1), pp. 1-11, 2021. doi: 10.1038/s41598-021-86950-4.

[10] Kayal, S. & Chakraborty, A., *Activated Carbon (Type Maxsorb-III) and MIL-101(Cr) Metal Organic Framework Based Composite Adsorbent for Higher CH_4 Storage and CO_2 Capture,* Chem. Eng. J., **334**, pp. 780-788, 2018. doi: 10.1016/j.cej.2017.10.080.

[11] Liu, X.Y., Huang, M., Ma, H.L., Zhang, Z.Q., Gao, J.M., Zhu, Y.L., Han, X.J. & Guo, X. Y., *Preparation of a Carbon-based Solid Acid Catalyst by Sulfonating Activated Carbon in A Chemical Reduction Process*, Molecules, **15**(10), pp. 7188-7196, 2010. doi: 10.3390/molecules15107188.

[12] Shi, L., Wang, X., Lu, L., Yang, X. & Wu, X., *Preparation of TiO_2/Polyaniline Nanocomposite from A Lyotropic Liquid Crystalline Solution*, Synth. Met., **159**(23-24), pp. 2525-2529, 2009. doi: 10.3390/molecules15107188.

[13] Mylarappa, M., Lakshmi, V.V., Mahesh, K.R.V., Nagaswarupa, H.P. & Raghavendra, N., *A Facile Hydrothermal Recovery of Nano Sealed MnO_2 Particle from Waste Batteries: An Advanced Material for Electrochemical and Environmental Applications*, IOP Conf. Ser.: Mater. Sci. Eng., **149**(1), 012178, 2016. doi: 10.1088/1757-899X/149/1/012178.

[14] Long, D. A., *Handbook of Vibrational Spectroscopy*, Volumes 1-5. Edited by Chalmers, J. M. & Griffiths, P. R., John Wiley & Sons, p. 3862, 2005.
[15] Belardi, G., Ballirano, P., Ferrini, M., Lavecchia, R., Medici, F., Piga, L. & Scoppettuolo, A., *Characterization of Spent Zinc-Carbon and Alkaline Batteries by SEM-EDS, TGA/DTA and XRPD Analysis*, Thermochim. Acta, **526**(1-2), pp. 169-177, 2011. doi: 10.1016/j.tca.2011.09.012.
[16] Kursunoglu, S. & Kaya, M., *Dissolution and Precipitation of Zinc and Manganese Obtained from Spent Zinc-Carbon and Alkaline Battery Powder*, Physicochem. Probl. Miner. Process, **50**(1), pp. 41-55, 2014. doi: 10.5277/ppmp140104.
[17] Furukawa, Y., Ueda, F., Hyodo, Y., Harada, I., Nakajima, T., and Kawagoe, T., *Macromolecules,* **21**(5), pp. 1297-1305. 1988. doi: 10.1021/ma00183a020.
[18] Cochet, M., Louarn, G., Quillard, S., Buisson, J.P. & Lefrant, S., *Theoretical and Experimental Vibrational Study of Emeraldine in Salt Form*. Part II, J. Raman Spectrosc., **31**(12), pp. 1041-1049, 2000. doi: 10.1002/1097-4555(200012)31:12<1041::AID-JRS641>3.0.CO;2-R.
[19] Xing, W., Qiao, S.Z., Ding, R.G., Li, F., Lu, G.Q., Yan, Z.F. & Cheng, H. M., *Superior Electric Double Layer Capacitors Using Ordered Mesoporous Carbons*, Carbon N.Y., **44**(2), pp. 216-224, 2006. doi: 10.1016/j.carbon.2005.07.029.
[20] Wang, H., Lin, J. & Shen, Z.X., *Polyaniline (PANi) Based Electrode Materials for Energy Storage and Conversion*, J. Sci. Adv. Mater. Devices, **1**(3), pp. 225-255, 2016. doi: 10.1016/j.jsamd.2016.08.001.
[21] Mishra, N., Shinde, S., Vishwakarma, R., Kadam, S., Sharon, M. & Sharon, M., *MWCNTs Synthesized from Waste Polypropylene Plastics and Its Application in Super-capacitors*, AIP Conf. Proc., **1538**(1), pp. 228-236, 2013. doi: 10.1063/1.4810063.
[22] Rustamaji, H., Prakosi, T., Devianto, H., Widiatmoko, P. & Nurdin, I., *Design, Fabrication, and Testing of Supercapacitor Based on Nanocarbon Composite Material*, ASEAN Journal of Chemical Engineering, **22**(1), pp. 19-32, 2022. doi: 10.22146/ajche.70139.
[23] Kumar, A., Rani S., and Chand S., *Expanded Conformation of Macromolecular Chain in Polyaniline Nanorods*, Appl. Phys. Lett., **89**(10), 103110, 2006. doi: 10.1063/1.2345376.
[24] Torre, C., Grossman, J., Bobko, A., and Bennewitz, M., *Tuning the Size and Composition of Manganese Oxide Nanoparticles through Varying Temperature Ramp and Aging Time*, PLOS ONE, **15**(9), e0239034, 2020. doi: 10.1371/journal.pone.0239034.
[25] Liu, X.-M., Fu, S.-Y., and Huang, C.-J., *Synthesis, Characterization and Magnetic Properties of β-MnO_2 Nanorods*, Powder Technology, **154**(2-3), 120-124, 2005. doi: 10.1016/j.powtec.2005.05.004.

[26] Devi, R., Kumar, V., Kumar, S., Bulla, M., Sharma, S., & Sharma, A. *Electrochemical Analysis of MnO_2 (α, β, and γ)-based Electrode for High-Performance Supercapacitor Application*, Applied Sciences, **13**(13), 7907, 2019. https://doi.org/10.3390/app13137907.

[27] Kaushal, I., Sharma, A. K., Saharan, P., Sadasivuni, K. K., and Duhan, S., *Superior Architecture and Electrochemical Performance of MnO_2 Doped PANI/CNT Graphene Fastened Composite*, Journal of Porous Materials, **26**(5), 1287-1296, 2019. doi: 10.1007/s10934-019-00728-8.

[28] Simotwo, S. K., DelRe, C., and Kalra, V., *Supercapacitor Electrodes Based on High-Purity Electrospun Polyaniline and Polyaniline–Carbon Nanotube Nanofibers*, ACS Applied Materials & Interfaces, **8**(33), 21261-21269, 2016. doi: 10.1021/acsami.6b03463.